**SUPPLEMENTAL MATERIALS FOR**
# *Trans*-splicing enhances translational efficiency in *C. elegans*

Y.-F. Yang, X. Zhang, X. Ma, T. Zhao, Q. Sun, Q. Huan, S. Wu, Z. Du, and W. Qian

Supplemental Materials include Supplemental Methods, Supplemental References, Supplemental Tables S1-10, and Supplemental Figures S1-9.

## SUPPLEMENTAL METHODS

### Sucrose gradient ultracentrifugation and fraction collection

The frozen worms were crushed with a mortar and pestle in a liquid nitrogen bath, and the resulting powder was transferred to three volumes of ice-cold polysome lysis buffer (200 mM Tris pH 8.0, 200 mM KCl, 35 mM $MgCl_2$, 1% Triton, 5 mM DTT, 100 μg/ml cycloheximide, and 0.5 mg/ml Heparin). After thawing on ice, the extract was centrifuged at 20,000 g for 10 min at 4°C. The supernatant was collected.

Ribosomes in the supernatant was enriched by centrifugation at 33,500 rpm (TY 70Ti rotor, Beckman) for 18 hours through a sucrose cushion. The sucrose cushion contains 400 mM Tris pH 9.0, 200 mM KCl, 35 mM $MgCl_2$, 60% (w/v) sucrose, 5 mM DTT, and 100 μg/ml Cycloheximide. The ribosome pellets were resuspended in resuspension buffer (200 mM Tris pH 9.0, 200 mM KCl, 35 mM $MgCl_2$, 5 mM DTT, and 100 μg/ml cycloheximide).

The dissolved ribosomes were separated through a 5%–50% sucrose gradient (40 mM Tris pH 8.0, 20 mM KCl, 10 mM $MgCl_2$, and 10 μg/ml cycloheximide, generated by the Gradient Master, BioComp) by centrifugation at 35,300 rpm for 3 h at 4°C (SW41Ti rotor, Beckman). The gradient was then fractionated by the Piston Gradient Fractionator (BioComp), and the absorbance at 254 nm was detected by the Model EM-1 Econo UV Monitor (BioRad).

### RNA extraction and RT-qPCR (reverse transcription and quantitative PCR)

Total RNA was extracted from each sucrose fraction with hot acidic phenol assay. Specifically, 75 μl 10% SDS and 750 μl phenol/chloroform/isoamyl alcohol (25:24:1, pH < 5.0) was added to each fraction of sample. The mixture was incubated at 65°C for 5 minutes with vortex, and was kept on ice for another 5 minutes. Supernatant was separated from the organic phase by centrifugation at 16,000 g for 15 min. RNA was precipitated from the supernatant by adding 1 μl glycogen (Invitrogen, AM9516), 1/10 volume 3 M ammonium acetate, and 1 volume of 100% isopropyl alcohol. RNA was resuspended in 10 μl nuclease-free water.

To synthesize complementary DNA (cDNA), 2 μg total RNA of each sample was reverse transcribed with GoScript™ Reverse Transcriptase (Promega, A5001) with random hexamers. The product was inactivated at 70°C for 15 minutes and was 10-fold diluted with nuclease-free water. Quantitative PCR was performed on Mx3000P qPCR System (Agilent Technologies) with Maxima SYBR Green/ROX qPCR Master Mix (Thermo Scientific, K0221).

In principle, we could also perform RNA-seq in each fraction to quantify the SL1/Non-SL ratio. However, because only a small proportion of sequencing reads (those covering trans-splicing sites) are informative, we chose to use qPCR instead.

**Generation of SL1 *trans*-splicing mutants**

We used the CRISPR-Cas9 system to remove the consensus sequence of *trans*-splicing sites of the *GFP* fusion genes in strains JH3203, JH3205, and JH3207, respectively. The guide sequences and their potential off-target sites were predicted using the CRISPR Design Tool (http://crispr.mit.edu/). Two guide sequences targeting two digesting sites were designed for each gene (Supplemental Table **S4**). To construct the sgRNA expression plasmids, the guide sequences were introduced into pDD162 plasmid (Addgene plasmid # 47549) by circular PCR (Supplemental Table **S5**) following previous protocols (Paix et al. 2014). The amplification products were digested by DpnI (NEB, R0176V) and were transfected into *E. coli* strain DH5α. Repair template sequences were designed to remove *trans*-splicing sites (Fig. **4C**). These sequences (Supplemental Table **S6**) contain ~400bp homologous sequences for efficient repair and were inserted into pPD95.77 (Addgene plasmid # 37465) plasmid (between AgeI and PstI restriction sites). A KpnI restriction site was designed within repair templates, for the purpose of efficient mutant screening.

Before worm transfection, all plasmids were purified with the PureLink PCR Micro kit (Invitrogen, K310050). For each strain, two Cas9-sgRNA plasmids, a repair template plasmid, and an editing reporter plasmid pRF4 (causing roller phenotype) were mixed and injected into the distal arm of the gonad at a final concentration of 50 ng/μl each. Roller F1 worms were recognized at the L4 stage and individual worms were separately transferred onto new plates. After laying enough eggs, single F1 worm on each plate was transferred into lysis buffer (1×PCR buffer, 1 μg/μl proteinase K) for genomic DNA extraction. The Cas9 targeting region was identified by single worm PCR in combination with following KpnI digestion (Supplemental Table **S7**). The mutation status of the target sites were further confirmed by DNA sequencing. For each gene, two individual SL1 *trans*-splicing site deletion strains were obtained.

It is also worth noting that the removal of the *trans*-splicing site TTTCAG in three SL1 mutants may also lead to the change of other sequence features. For example, although the Kozak context in the *lin-15B* and *deps-1* mutants kept largely unchanged, the Kozak context of *mes-2* significantly altered, which may also contribute to the decreased translational efficiency (Fig. **4C**). It was also possible in principle that the mutations generated on SL1 *trans*-splicing sites and surrounding regions (e.g., silent mutations to prevent Cas9 from re-cutting) created new stable mRNA secondary structures in the non-*trans*-spliced transcripts of SL1 mutants. To examine this possibility, we calculated the sMFEs of these transcripts and confirmed that stable secondary structure was not

introduced in these mutants. Taken together, the results of three reporter genes suggest that the removal of uAUG and stable structures are likely important determinants of SL1 *trans*-splicing mediated translational regulation.

**Measuring the SL1 *trans*-splicing frequency for *GFP* fusion genes**

Worms were collected and immediately frozen at -80°C in two volumes of lysis buffer (200 mM Tris pH 8.0, 200 mM KCl, 35 mM $MgCl_2$, 1% Triton, 5mM DTT). The pellets were thawed, mixed, and refrozen in liquid nitrogen for three times. After that, RNA was isolated by hot acidic phenol assay and was quantified by qPCR (Supplemental Table **S8**). We used the ratio of (non-*trans*-spliced / total) rather than the ratio of (SL1 *trans*-spliced / total) to quantify the SL1 *trans*-splicing frequency (Supplemental Fig. **S7**) for two reasons. First, because the SL1 sequence is shared by thousands of transcripts in the genome, using it as the upstream primer to amplify SL1 *trans*-spliced transcripts leads to reduced amplification specificity, and thus inaccurate RNA quantification. Second, because SL1 *trans*-splicing may take place at multiple sites in SL1 mutants, we could not design specific primers as we did in Fig. **3B**. When comparing total mRNA levels of the reporter genes between the wild-type and SL1 mutants, the mRNA abundance of *GFP* was normalized to a tubulin gene (*tba-1*) (Supplemental Fig. **S7** and Supplemental Table **S8**). For each genotype, two biological replicates and three technical replicates were performed.

**Image collection and quantification**

Embryos were mounted following a well-established protocol with minor modifications (Bao and Murray 2011). Briefly, embryos were collected and mounted in M9 buffer (22 mM $KH_2PO_4$, 42 mM $Na_2HPO_4$, 85 mM NaCl, 1 mM $MgSO_4$) containing 20 μm microspheres (Polyscience, Warrington, PA), and were sealed between two cover slips. Fluorescence micrographs were taken using spinning disk confocal microscopy (Perkin Elmer) with Hamamatsu Flash4.0 and 9100-23B cameras. Images of the center focal plane were acquired and GFP intensities were quantified by ImageJ. Average intensity was measured in cells (*deps-1*) or an entire embryo (*lin-15B* and *mes-2*) with the background signal subtracted, which was estimated as the average intensity of three randomly picked areas in the same image without a visible fluorescence signal.

**Phenotype analysis**

**Lifetime fecundity**: Single worms were grown on plates at 21°C and the total number of viable animals in the F1 generation was used to measure lifetime fecundity. Animals were transferred daily till the cease of egg-laying. Viable offspring were counted one day after each parent transfer.

**Embryonic lethality**: More than 100 eggs were obtained by allowing 5-10 adult worms to lay eggs for one day on plates at 21°C. Parent worms were then removed. The proportion of embryos that failed to hatch in one day was estimated.

**Sterility**: About 50 synchronized L1 stage worms were grown on plates at 21°C for three days. Worms without eggs in the uterus were defined as sterile animals.

**Definition of one-to-one orthologous genes with difference in *trans*-splicing status**

We observed more *trans*-spliced genes in *C. elegans* than in the other three species (Supplemental Fig. **S4**), which we believe is an experimental artifact for the following reasons. SL1 *trans*-splicing may be subject to regulation itself, and thus, transcriptomic data in more developmental stages and environments facilitate a more thorough identification of SL1 *trans*-spliced genes. Indeed, compared to the other 3 nematode species, the transcriptome of *C. elegans* has been examined in more developmental stages and under more environmental perturbations (Allen et al. 2011). Therefore, to avoid false discovery of orthologous genes with *trans*-splicing turnover, we focused on the one-to-one orthologous genes with SL1 *trans*-splicing evidence in *C. briggsae*, *C. remanei*, or *C. brenneri*, but without *trans*-splicing evidence in *C. elegans* (Fig. **2**).

**Calculation of initiation score**

RNA sequences around the start codons of annotated open reading frames (ORFs) were extracted from the *C. elegans* genome, and a sequence logo was created (Fig. **S2A**) with WebLogo (Schneider and Stephens 1990; Crooks et al. 2004). Consensus sequences were observed at the positions -3 to -1 relative to the first base of the start codon, which was consistent with previous studies (Ramani et al. 2009). Thus, for each gene, sequences at position -3 to -1 were used to estimate an "initiation score", which measures the similarity of a sequence to the consensus Kozak sequence. The initiation score of each gene was calculated as follows. First, the uncertainty of position *i* ($H_i$) was calculated:

$$H_i = -\sum_{1}^{4} f_{N,i} \times \log_2 f_{N,i}$$

where $f_{N,i}$ is the fraction of base *N* (one of A, C, G, and U) at position *i* (in [-3, -1]) among all annotated ORFs. Second, the information content at position *i* ($R_i$) of a specific sequence was given by:

$$R_i = (2 - H_i) \times f_{S,i}$$

where *S* is the base at position *i* in the sequence. The initiation score of the sequence is defined as the sum of $R_i$:

$$initiation\ score = \sum_{i=-3}^{-1} R_i$$

**Codon adaptation index (CAI)**

Synonymous codons are used with bias in the *C. elegans* genome. Following Sharp and Li (1987), we calculated the CAI, which measures the codon usage similarity of a gene to a set of 1,000 most highly expressed genes in *C. elegans* (Supplemental Table **S10**). The relative synonymous codon usage of codon *k* encoding amino acid *m* ($RSCU_{k,m}$) in these 1,000 genes was calculated as follow

$$RSCU_{k,m} = \frac{n_m \times N_{k,m}}{N_m}$$

where $N_{k,m}$ is the number of codon *k* among these 1,000 genes, $N_m$ is the amino acid *m* among these 1,000 genes, and $n_m$ is the number of synonymous codons of amino acid *m*. The CAI of a gene was calculated by the following equation:

$$CAI = \sqrt[L]{\prod_{i=1}^{L}(RSCU_i/RSCU_{imax})}$$

where $RSCU_i$ is the *RSCU* value of the codon at position *i* of a gene and *L* is the total number of codons in the gene. $RSCU_{imax}$ is the maximum *RSCU* value of the amino acid encoded by the codon at position *i*.

**Minimum free energy (MFE)**

The MFE in a 5' UTR was estimated with RNAfold version 2.1.8 (Lorenz et al. 2011). Because of the inequality of 5' UTR lengths among genes, a sliding window was used (size 22 nt, step 1 nt). The length of 22-nucleotides was used because it is the shortest 5' UTR length after SL1 *trans*-splicing. The smallest MFE among all the sliding windows in a 5' UTR was used as the folding energy of the most stable secondary structure.

## SUPPLEMENTAL REFERENCES


Allen MA, Hillier LW, Waterston RH, Blumenthal T. 2011. A global analysis of *C. elegans trans*-splicing. *Genome Res* **21**(2): 255-264.

Bao Z, Murray JI. 2011. Mounting *Caenorhabditis elegans* embryos for live imaging of embryogenesis. *Cold Spring Harb Protoc* **2011**(9).

Crooks GE, Hon G, Chandonia JM, Brenner SE. 2004. WebLogo: a sequence logo generator. *Genome Res* **14**(6): 1188-1190.

Lorenz R, Bernhart SH, Honer Zu Siederdissen C, Tafer H, Flamm C, Stadler PF, Hofacker IL. 2011. ViennaRNA Package 2.0. *Algorithms Mol Biol* **6**: 26.

Paix A, Wang Y, Smith HE, Lee CY, Calidas D, Lu T, Smith J, Schmidt H, Krause MW, Seydoux G. 2014. Scalable and versatile genome editing using linear DNAs with microhomology to Cas9 Sites in *Caenorhabditis elegans*. *Genetics* **198**(4): 1347-1356.

Ramani AK, Nelson AC, Kapranov P, Bell I, Gingeras TR, Fraser AG. 2009. High resolution transcriptome maps for wild-type and nonsense-mediated decay-defective *Caenorhabditis elegans*. *Genome Biol* **10**(9): R101.

Schneider TD, Stephens RM. 1990. Sequence logos: a new way to display consensus sequences. *Nucleic Acids Res* **18**(20): 6097-6100.

**SUPPLEMENTAL TABLES**

**Supplemental Table S1. Primers used for qPCR in polysome profiling experiments in Figure 3.**

| Primer | DNA Sequence (5'-3') |
|---|---|
| **CE05167-S-F** | cccaagtttgagTTTCCATCA[1] |
| **CE05167-SN-R** | GCTCGTCGAAGTCACCATT |
| **CE05167-N-F** | tgtttttgtatcagTTTCCATCA |
| | |
| **CE09020-S-F** | caagtttgagTTGATTCATTC |
| **CE09020-SN-R** | TCACATCCCGGATCACAAA |
| **CE09020-N-F** | ctgtttatttagTTGATTCATTCA |
| | |
| **CE13385-S-F** | tacccaagtttgagGCTTTGA |
| **CE13385-SN-R** | TCGCTTCATAGTCTTCGCCA |
| **CE13385-N-F** | agtttccagGCTTTGAATATGGA |
| | |
| **CE16053-S-F** | ccaagtttgagGCTTATATCACA |
| **CE16053-SN-R** | TGGATGCTCTGGATCGTTGA |
| **CE16053-N-F** | gcttaatttccagGCTTATATCAC |
| | |
| **CE16882-S-F** | acccaagtttgagCTGAAATGC |
| **CE16882-S-R** | CGAGTACGCATCGCTTAATGT |
| **CE16882-N-F** | cgaaaatcttttacagCTGAAATGC |
| **CE16882-N-R** | TCCGCAATCGTTCGAAATCA |
| | |
| **CE19166-S-F** | tacccaagtttgagATTACT |
| **CE19166-SN-R** | TTGCGTGGCTGTATTGTG |
| **CE19166-N-F** | ttgccattatacagATTACTC |
| | |
| **CE19511-S-F** | cccaagtttgagAAAGACTACTG |
| **CE19511-S-R** | TCAGCGGTAATTGATGAGGAGA |
| **CE19511-N-F** | gaaattttcagAAAGACTACT |
| **CE19511-N-R** | GAATACCTCATGAAGAACTG |
| | |
| **CE22417-S-F** | ttacccaagtttgagAATCACA |
| **CE22417-SN-R** | TTCCCATGTTCCATCTCCAA |
| **CE22417-N-F** | ttttgcttgcagAATCACACA |
| | |
| **CE27244-S-F** | ttacccaagtttgagACACA |
| **CE27244-SN-R** | TTGGGCCCATAGTGACAGA |
| **CE27244-N-F** | tttttcagACACAAAAGATGCTT |
| | |
| **CE31579-S-F** | ccaagtttgagGGAATATCGGTCT |
| **CE31579-SN-R** | GCTTTCAATACCTTAGCCGCA |

| | |
|---|---|
| **CE31579-N-F** | ttcgcagGGAATATCGGTCT |
| | |
| **CE34242-S-F** | ccaagtttgagCCATGACAA |
| **CE34242-SN-R** | TCTTGAAGGCACGAAGACAA |
| **CE34242-N-F** | ttataatttagCCATGACAATTC |
| | |
| **CE34630-S-F** | cccaagtttgagTGCTGTTC |
| **CE34630-S-R** | TCTACCATGTCGAGCCAACA |
| **CE34630-N-F** | ttgttcagTGCTGTTCAAAC |
| **CE34630-N-R** | TTTCTACCATGTCGAGCCAA |

[1] SL1 or non-*trans*-spliced specific sequences are in lower case.

**Supplemental Table S2. Strain information**

| Strain | Genotype | Description |
|---|---|---|
| **JH3203** | *mes-2(ax2059[mes-2::GFP]) II* | *GFP* was inserted at the 3'-terminus of *mes-2*. |
| **SYS39** | *mes-2(dev22), mes-2(ax2059[mes-2::GFP]) II* | *Trans*-splicing site of *mes-2* (TTTCAG, 1 bp upstream of start codon) was removed by CRISPR-Cas9. |
| **JH3205** | *lin-15B(ax2061[lin-15B::GFP]) X* | *GFP* was inserted at the 3'-terminus of *lin-15B*. |
| **SYS24** | *lin-15B(dev8), lin-15B(ax2061[lin-15B::GFP]) X* | *Trans*-splicing site of *lin-15B* (TTTCAG, 6 bp upstream of start codon) was removed by CRISPR-Cas9. |
| **JH3207** | *deps-1(ax2063[deps-1::GFP]) I* | *GFP* was inserted at the 3'-terminus of *deps-1*. |
| **SYS42** | *deps-1(dev25), deps-1(ax2063[deps-1::GFP]) I.* | *Trans*-splicing site of *deps-1* (TTTCAG, 6 bp upstream of start codon) was removed by CRISPR-Cas9. The mutants exhibited partial embryonic lethality and some adults were sterile. The mutants were maintained at 20˚C. |

**Supplemental Table S3. The 5' UTRs of pre-mRNA and SL1 *trans*-spliced mRNA of three reporter genes.**

| Gene | 5' UTR of pre-mRNA[1] | 5' UTR of SL1 *trans*-spliced mRNA |
|---|---|---|
| *lin-15B* | ACTTGCCTCACGCTCTCTACTCTCTCGTTC CCGCATTGTATTTCCTCTCGCACGCAGAT TTGAAAATTTATAATAAACGCACAAAAT TATGTGCTTTTTTCGTTGAATTCGAGTGA ACATTTTGAAGTTTTCAGTCAAGTAAAAG TTGTAGAATTCAAATATTCACCGTTTTTT TTTCGGTTAACTTTTATTTTCAAATAATA ATGACTTTTTAACCATTCTATCATCTTGTT CTTAGCGTATTGTATCCTACCGTACTTCC TGATTAAACTTGTTGTCTTTCTACACGTA TTACCTTGCATGATGACCGAATAATTTAT TATTTTTTTTATATTTTCAGGTAATT | GGTTTAATTACCCA AGTTTGAGGTAATT |
| *mes-2* | ACTTGCAATGTTTTTAAAAATTAAAAATT GTTTGTTTTCGATTTATTCTCTCGTCTTTT TCGTCTTAATACAATTTTCTCCCTTTTTAA AACGCAATATTCTTTCAGA | GGTTTAATTACCCA AGTTTGAGA |
| *deps-1* | ACTGCGCCGCGCATCTGATTTCTCGTGGG AAATTTGTTTCGAATCCTACGTTTTTTAC AGATTTTTCTTTTTTTTCGTTTCGCTCATC ATTTTTTTGTTGCAAAAAATCCAATTTTC AGACAAAA | GGTTTAATTACCCA AGTTTGAGACAAAA |

[1] The 5' UTRs in the wild-type were inferred from the transcription start sites identified in the SL1 mutants.

**Supplemental Table S4. Guide sequences used for knocking out the consensus sequence of *trans*-splicing sites by CRISPR-Cas9.**

| Sequence name | Target gene | Guide sequences (5'-3') |
|---|---|---|
| **JH3203-1** | *mes-2::GFP* | AAGAATATTGCGTTTTAAAAAGG |
| **JH3203-2** | *mes-2::GFP* | CCTGAGGGAGTTGATGTGCTGGG |
| **JH3205-1** | *lin-15B::GFP* | AATTATTCGGTCATCATGCAAGG |
| **JH3205-2** | *lin-15B::GFP* | AGCACGACTTACATCAAACCCGG |
| **JH3207-1** | *deps-1::GFP* | CCGCGCATCTGATTTCTCGTGGG |
| **JH3207-2** | *deps-1::GFP* | GATAGTCAAAATATTTGGATTGG |

**Supplemental Table S5. Primer sequences used for Cas9-sgRNA plasmid construction.**

| Primer name | Primer sequence (5'-3') |
|---|---|
| **JH3203-1-F** | AGAATATTGCGTTTTAAAAGTTTTAGAGCTAGAAATAGC |
| **JH3203-1-R** | TTTTAAAACGCAATATTCTCAAGACATCTCGCAATAGGA |
| **JH3203-2-F** | CTGAGGGAGTTGATGTGCTGTTTTAGAGCTAGAAATAGC |
| **JH3203-2-R** | AGCACATCAACTCCCTCAGCAAGACATCTCGCAATAGGA |
| **JH3205-1-F** | ATTATTCGGTCATCATGCAGTTTTAGAGCTAGAAATAGC |
| **JH3205-1-R** | TGCATGATGACCGAATAATCAAGACATCTCGCAATAGGA |
| **JH3205-2-F** | GCACGACTTACATCAAACCGTTTTAGAGCTAGAAATAGC |
| **JH3205-2-R** | GGTTTGATGTAAGTCGTGCCAAGACATCTCGCAATAGGA |
| **JH3207-1-F** | CGCGCATCTGATTTCTCGTGTTTTAGAGCTAGAAATAGC |
| **JH3207-1-R** | ACGAGAAATCAGATGCGCGCAAGACATCTCGCAATAGGA |
| **JH3207-2-F** | ATAGTCAAAATATTTGGATGTTTTAGAGCTAGAAATAGC |
| **JH3207-2-R** | ATCCAAATATTTTGACTATCAAGACATCTCGCAATAGGA |

**Supplemental Table S6. Repair template sequences used for knocking out the consensus sequence of *trans*-splicing sites by CRISPR-Cas9.**

| Sequence name | Sequence (5'-3') |
|---|---|
| **JH3203-repair** | GGGTAACATATTTTGCAAAAAGCATTTGGTTTTCCT<br>TGTCAGATTCAAATTCCAAACCTTCGCGCCAACTTC<br>ACATTATCAATAGGGCGCGATTGCACGCAACACTT<br>GCAATGTTTTTAAAAATTAAAAATTGTTTGTTTTCG<br>ATTTATTCTCTCGTCTTTTTCGTCTTAATACAATTTT<br>CTGGTACCTTAAAACGCAATATTCAATGAGCAACTC<br>AGAGCCTAGTACTTCTACTCCCTCAGGAAAAACAA<br>AGAAGCGCGGGAAAAAGTGCGAAACTTCTATGGGA<br>AAATCGAAGAAATCGAAAAATTTGCCTCGCTTTGT<br>GAAAATTCAGCCAATTTTTTCATCTGAAAAAATCAA<br>GGAGACCGTGTGCGAACAAGGAATTGAAGAATGTA<br>AACGTATGCTTAAAGGCCACTTC |
| **JH3205-repair** | CAGTCAAGTAAAAGTTGTAGAATTCAAATATTCAC<br>CGTTTTTTTTTCGGTTAACTTTTATTTTCAAATAATA<br>ATGACTTTTTAACCATTCTATCATCTTGTTCTTAGCG<br>TATTGTATCCTACCGTACTTCCTGATTAAACTTGTTG<br>TCTTTCTACACGTATTACGGTACCTGATGACCGAAT<br>AATTTATTATTTTTTTTATATGTAATTATGCAAACGC<br>TAAAAACAGCACGACTTACTTCTAACCCTGCATCA<br>ATTCCGACTTCCAGCAGTAGCAGTGCAATGTACGTT<br>TATTCTTGATTGATAATTTTCTATTCCAAATGCATTC<br>CAACCACATTCAACAAAACATATTTTTTCAGAAGCG<br>CAGCAGCAATTCAAAAGACGCTTGATGCCGTGAAT<br>CGCCCACCAGCAGTCAG |
| **JH3207-repair** | CAGAAAAAATAAGTTTTAAAACAGAATTTTAATGG<br>AAAAATAAACGGAAAAATTCGAAACTTTTTTTTCCG<br>CCATTGAACACCAATGTGCCTTTAAGGTACGGTAGC<br>TCTTCGTGGTGAGACCACTGCGCCGCGCATCTGATT<br>TCTGGTACCAAATTTGTTTCGAATCCTACGTTTTTTA<br>CAGATTTTTCTTTTTTTTCGTTTCGCTCATCATTTTTT<br>TGTTGCAAAAAATGAATTCCAAAAATGTCAGAACG<br>GCAGTCGAAATATTTTGACTATCAAGGTATCGTCAT<br>TTCCTCCACTGGACAAGATAACCAAGATTCGGAGA<br>CGGACCTCGTTTATCTCATTCAAGCTCATGTACGTG<br>AATTCCCTCCGTTTTCATATTTAAAATAATAAGCTC<br>GTTTTCAGGGAAAAGCGGC |

**Supplemental Table S7. Primer sequences used for worm screening after knocking out the consensus sequence of *trans*-splicing sites with CRISPR-Cas9.**

| Primer name | Primer sequence (5'-3') |
|---|---|
| **JH3203-scr-F** | ATTCGATGAAAACTCCGCGG |
| **JH3203-scr-R** | GCTCGCATCCTTCAACCAAT |
| **JH3205-scr-F** | CTACTCTCTCGTTCCCGCAT |
| **JH3205-scr-R** | CAGGAAAGCTGGCTCATGTG |
| **JH3207-scr-F** | ACTTGATCGAAAAGCCAGCG |
| **JH3207-scr-R** | TCCATAGGATGACTTCACCGAACT |

**Supplemental Table S8. Primer sequences for qPCR in Supplemental Figure S7.**

| Primer name | Primer sequence (5'-3') |
|---|---|
| **JH3203-nonSL1-F** | GTTTTCGATTTATTCTCTCGTC |
| **JH3203-nonSL1-R** | CGATTTTCCCATAGAAGTTTCGC |
| **JH3205-nonSL1-F** | TCCTACCGTACTTCCTGATT |
| **JH3205-nonSL1-R** | ACTGCTGGAAGTCGGAATTG |
| **JH3207-nonSL1-F** | CGTTTCGCTCATCATTTTTTTGTTGC |
| **JH3207-nonSL1-R** | GAGATAAACGAGGTCCGTCTCCGAATC |
| **GFP-F** | ATGGCCCTGTCCTTTTACCA |
| **GFP-R** | CCATGTGTAATCCCAGCAGC |
| **Tubulin-F** | GAGCCAACTGTTGTTGATGAGATC |
| **Tubulin-R** | CTGCAGTTGTCAGCGAGGCGACG |

**Supplemental Table S9. Primer sequences used for 5’ RACE.**

| Primer name | Primer sequence (5'-3') |
|---|---|
| **JH3205-RACE** | GATTACGCCAAGCTTGCATTGTTGAAGAAGGCGCTGGAGGT |
| **JH3203-RACE** | GATTACGCCAAGCTTCGGGCGCTCACATTTTCTGCCATCGA |
| **JH3207-RACE** | GATTACGCCAAGCTTGGCAGGAACGACGCGGGTAAGGAGAT |

**Supplemental Table S10. One thousand most highly expressed genes used for calculating CAI.**

| | | | | |
|---|---|---|---|---|
| K12G11.3 | Y73B3A.18 | F48D6.4 | C31E10.7 | F08B6.2 |
| R03G5.1 | K06G5.1 | K08C7.3 | F46A9.5 | T28B11.1 |
| T04C12.6 | W05G11.6 | F23B2.5 | C26D10.2 | T23H2.2 |
| T27E9.1 | H19M22.2 | W02F12.5 | C18H7.1 | T20H4.5 |
| ZC247.1 | K07C5.4 | Y54F10AM.8 | D2013.7 | C12D12.2 |
| F13B10.2 | ZK455.1 | VW06B3R.1 | H05L03.3 | H17B01.4 |
| C34E10.6 | R53.4 | F57F5.1 | ZK112.1 | C17F4.7 |
| M03F4.2 | C29F4.1 | F55H2.6 | Y39G10AR.8 | K06A5.6 |
| F26D10.3 | T25B9.9 | F46F11.5 | Y51F10.7 | Y38F2AR.2 |
| F11C3.3 | W09C5.8 | R12B2.5 | C05D11.11 | C06G3.5 |
| C05E4.9 | K07E12.1 | ZK1320.9 | VW02B12L.1 | H16D19.1 |
| H28O16.1 | F54F11.2 | T27E9.7 | Y54G11A.5 | C53C9.2 |
| B0041.4 | C37H5.8 | R119.4 | C41G7.9 | W10D5.2 |
| R11A5.4 | F54H12.6 | ZK945.3 | F35B12.9 | C54D1.5 |
| B0250.1 | R09B5.6 | Y48G9A.3 | M7.1 | T08B2.9 |
| F57F4.4 | T10E10.5 | Y113G7B.17 | Y37D8A.2 | M04G7.1 |
| F57F4.3 | F54C1.7 | C28H8.3 | E01A2.10 | Y49A3A.5 |
| F53G12.10 | T05D4.1 | F43G9.1 | Y69F12A.2 | Y69H2.3 |
| F10B5.1 | C25A1.10 | Y87G2A.5 | D2030.2 | T02C12.1 |
| C23G10.3 | F29D11.1 | T05H10.6 | K02D7.4 | F10G7.1 |
| ZC434.2 | C54C6.1 | F48E8.5 | C05G5.4 | T24A11.1 |
| C09D4.5 | K07H8.10 | F42A8.2 | Y71H10A.1 | K02F3.4 |
| Y57G11C.16 | Y37D8A.14 | T13F2.1 | W03F8.5 | C25F6.2 |
| R151.3 | F21F8.3 | C03G5.1 | C09B8.6 | ZK675.1 |
| F25H2.10 | Y105C5B.28 | F41C3.3 | F22B7.9 | W01A8.4 |
| F40F8.10 | F01G12.5 | F31C3.1 | R13A5.12 | F35B12.3 |
| Y43B11AR.4 | C49C3.4 | T05C12.7 | Y37E3.9 | C08F11.8 |
| F56F3.5 | T25C12.3 | F56C9.1 | C06G4.2 | C44E4.6 |
| B0393.1 | F27D9.5 | C42D4.1 | F25B4.9 | R57.1 |
| F54C9.5 | M01H9.3 | Y48B6A.14 | T05H4.5 | Y48A6B.3 |
| T20G5.2 | F08B6.4 | C18A11.7 | Y71F9AL.9 | F32G8.4 |
| F28D1.7 | D1025.9 | T10B5.5 | K10C2.4 | Y71H10A.2 |
| F42C5.8 | F49E2.5 | W10C8.5 | K11D2.2 | F27D4.4 |
| C47E8.5 | T10E10.6 | C14B9.1 | W06H8.6 | W03C9.3 |
| C14B9.7 | F25H5.3 | C06A8.1 | F19C7.1 | T25G3.3 |
| C32E8.2 | R06C7.10 | Y22D7AL.10 | F38H4.9 | F55C7.7 |
| M01F1.2 | F52E4.1 | R07E3.1 | C39F7.4 | ZK632.6 |
| C49H3.11 | F53F4.13 | K01C8.10 | F54D1.6 | T16G1.11 |
| R13A5.8 | Y16B4A.2 | T05H4.13 | Y119D3B.21 | M02D8.1 |
| F36A2.6 | W01B11.3 | T14F9.1 | B0035.7 | F08C6.1 |
| K04D7.1 | Y41E3.10 | Y55F3AR.3 | R151.2 | ZK742.1 |
| T07A9.11 | C47B2.3 | ZK484.2 | F15G9.4 | T10F2.1 |
| T04C12.5 | T22F3.11 | F23H11.5 | T17H7.4 | F32D1.2 |

| | | | | |
|---|---|---|---|---|
| ZK829.4 | T22B11.5 | Y51H4A.3 | T19A6.2 | F21F3.6 |
| E04A4.8 | Y71H2AM.5 | C25F6.3 | F23C8.5 | ZK856.7 |
| T28C6.6 | R144.7 | W07E11.1 | F36H1.6 | C16H3.2 |
| T05F1.3 | R10E11.2 | F29B9.11 | ZK970.4 | Y94H6A.10 |
| ZK1010.1 | ZK1151.1 | Y87G2A.8 | Y65B4BL.5 | F45E1.6 |
| Y71F9AL.13 | C53A5.1 | C53B7.4 | M60.2 | R13A1.2 |
| VC5.3 | C17H12.14 | F52B5.1 | F56B6.4 | F57B9.3 |
| F40F11.1 | K08D12.3 | F29C4.2 | C50F4.5 | Y71F9B.3 |
| F45D11.14 | T21H3.3 | C01F6.6 | F40F4.3 | ZK863.8 |
| K10B3.7 | C06A8.3 | K04G7.4 | Y71F9AL.17 | C41C4.8 |
| F54D8.3 | K07E3.4 | F01F1.8 | B0511.6 | ZK1005.1 |
| T24B8.1 | C36E8.5 | M6.1 | Y71G12B.11 | T23H2.1 |
| K11H12.2 | F40F4.6 | F28H1.2 | K04E7.2 | C02E11.1 |
| F45D11.16 | W02D3.5 | T08G11.1 | T05C3.5 | F49C12.13 |
| K02F2.2 | F42G8.12 | C14B1.1 | F53G12.1 | B0432.4 |
| D1007.12 | C51E3.7 | K07A3.1 | T16G12.1 | C45G9.6 |
| Y37E3.8 | T21H3.1 | C30G7.1 | C23H3.4 | F21D5.7 |
| F54H12.1 | W08E12.7 | C01G8.5 | T25C12.1 | T09B4.8 |
| F07D10.1 | D1037.3 | T13C2.6 | F13D12.2 | F55C5.8 |
| ZK973.6 | M28.5 | F28A12.4 | C31C9.1 | K11G9.6 |
| K10B3.8 | ZK822.4 | Y24D9A.8 | Y111B2A.18 | F09G2.9 |
| C44B7.10 | F36A2.7 | ZC434.5 | C50F4.13 | T10E9.7 |
| F46H5.3 | F56H11.4 | R10E4.2 | B0491.5 | R01E6.3 |
| F28F8.2 | C56G2.6 | C10G8.5 | Y43F4B.5 | R03E9.1 |
| T08B2.10 | F54D8.2 | R11H6.1 | F28H1.3 | T20B3.2 |
| Y38A10A.5 | K12F2.1 | ZK909.2 | C14B9.2 | F22D6.3 |
| T05E11.1 | F01D4.4 | T07C4.5 | T26A5.9 | F56F10.1 |
| Y24D9A.4 | F10C1.2 | ZC155.1 | Y54G11A.6 | C26C6.1 |
| JC8.3 | K04H4.1 | F35H10.4 | T03F1.11 | W05B2.6 |
| F37C12.9 | Y18D10A.19 | B0336.2 | Y46E12BL.2 | C24G6.6 |
| T25C8.2 | C53B7.3 | W01A8.1 | C33A11.1 | T07E3.6 |
| Y39B6A.20 | T01C8.5 | Y45G12B.1 | C25A11.4 | F53H10.2 |
| Y37E3.7 | Y67D8C.10 | Y66H1A.4 | F26F12.7 | F57B9.5 |
| F54C9.1 | W06H8.8 | T20D3.2 | F08B12.4 | C43C3.1 |
| K11D9.2 | T06D8.1 | Y38F1A.6 | T08H10.1 | Y32F6A.5 |
| C09H10.2 | C08E3.13 | F41G3.10 | F25B4.1 | Y42G9A.4 |
| Y48G8AL.8 | T21B6.3 | T22B7.3 | T01B11.2 | Y59A8A.3 |
| C53H9.1 | T22E5.5 | K02A4.1 | R10H10.3 | F01F1.6 |
| F25H2.5 | ZK721.2 | C01B10.6 | C35B1.5 | ZK632.9 |
| B0336.10 | F10G8.5 | F37B4.2 | ZK337.1 | T11B7.5 |
| F25B5.4 | T22F3.3 | T24H7.1 | C40H1.5 | R05D3.7 |
| Y82E9BR.3 | C23H4.1 | F58F12.1 | R166.5 | F45H10.2 |
| D1007.6 | ZK1127.10 | F53A2.7 | F57B10.14 | W04D2.1 |
| F01G4.6 | K04D7.3 | Y53G8AL.2 | F38E11.5 | T10H9.5 |
| K02B2.5 | T23D8.4 | M03A8.1 | R05F9.6 | F25H8.5 |
| ZK652.4 | Y38F2AL.3 | T21B10.7 | Y39A1C.3 | T05F1.1 |

| | | | | |
|---|---|---|---|---|
| F25H2.11 | K01A2.2 | T20G5.7 | C41D11.2 | F08C6.6 |
| H22K11.1 | F15E11.13 | T05H4.6 | B0310.5 | F42D1.2 |
| C04F12.4 | LLC1.3 | C15C8.3 | Y54G2A.32 | T03F6.1 |
| Y48B6A.2 | F09B12.3 | B0222.7 | ZK1073.1 | ZK328.2 |
| C42C1.14 | T02C5.1 | W01A11.4 | F35G12.2 | H15N14.2 |
| H06I04.4 | R07H5.8 | F57B10.3 | C18F3.2 | B0334.3 |
| C27A2.2 | T25F10.6 | C47D12.6 | Y73B6BL.24 | C44C10.1 |
| F39B2.6 | Y67H2A.5 | Y55B1AR.1 | F39B2.10 | F55B11.1 |
| F21F8.7 | Y73B6BL.6 | Y71H2AM.23 | H39E23.1 | C49H3.3 |
| T07H6.3 | C01G6.1 | C37C3.2 | R07E5.2 | C18A3.5 |
| F21C10.10 | F32A5.5 | F07B7.11 | K08F4.2 | K04G7.3 |
| C36A4.9 | F15E11.1 | C50C3.6 | Y17G7B.20 | Y22F5A.5 |
| F53A3.3 | C54G4.8 | H06I04.3 | Y18D10A.5 | Y39G10AR.11 |
| C16A3.9 | C07G2.3 | M163.3 | C46F4.2 | ZK1307.8 |
| B0222.8 | F44C4.3 | ZK54.2 | Y25C1A.5 | Y41E3.4 |
| C15H9.6 | M02F4.8 | F38A3.2 | Y37E3.10 | F54D5.8 |
| F56D12.5 | F54D11.1 | R08E3.1 | F58B3.5 | C23G10.4 |
| C26F1.4 | ZK617.1 | K08F8.1 | K02D7.1 | R09E12.3 |
| W09B6.1 | Y66H1B.2 | T03F1.3 | ZK829.7 | W03D2.1 |
| F52H3.7 | F52B5.6 | ZC412.3 | K04G2.1 | C14C10.4 |
| F57B9.6 | F58E10.3 | Y71F9AM.6 | C23F12.1 | F38A5.13 |
| C07A12.4 | C30C11.4 | B0511.10 | Y74C10AR.1 | T19E7.2 |
| F52D10.3 | K01G5.7 | R08D7.3 | Y105E8B.5 | C02D5.4 |
| H39E23.3 | F32E10.4 | F59C6.5 | F32D8.12 | ZK673.7 |
| Y45F10D.12 | M04G12.2 | ZK892.1 | ZK637.8 | ZK270.1 |
| T01C3.6 | T02H6.11 | K03A1.5 | M88.6 | F26H9.6 |
| F37C12.4 | F38A6.3 | R09B3.3 | T27F7.3 | C25A1.6 |
| F17C11.9 | C44E4.4 | F58G1.4 | K05F6.11 | F44E7.2 |
| F20H11.3 | Y57G11C.10 | H02I12.6 | C32F10.8 | F33A8.5 |
| F01F1.12 | F41C3.5 | F11E6.3 | F18H3.3 | F17E9.9 |
| B0513.3 | F14F7.1 | F44E5.1 | T14G11.3 | R155.1 |
| VZK822L.1 | F10G7.2 | R74.1 | F41E6.4 | C30F12.7 |
| D2096.8 | Y55H10A.1 | W03F8.1 | C06G1.4 | F15E11.15 |
| B0365.3 | Y75B12B.5 | F43E2.7 | C37H5.6 | Y45G12C.2 |
| Y106G6H.2 | ZC101.2 | F11C7.5 | T12A2.2 | B0244.2 |
| C26F1.9 | R05F9.12 | C04C3.3 | Y74C9A.2 | F22B8.6 |
| F28C6.7 | F54D5.3 | Y22F5A.4 | R05F9.10 | R05C11.3 |
| C53D5.6 | ZK1248.16 | F40F4.2 | H28G03.1 | C16A3.5 |
| H06O01.1 | C03B1.12 | H06H21.3 | Y46G5A.31 | C50F4.1 |
| F10C1.7 | K12H4.7 | T03D8.3 | W05B2.1 | C14C10.5 |
| F37C12.11 | K01G5.5 | R03E1.2 | ZK1058.2 | C25G4.10 |
| F10E7.7 | F23B12.5 | T22D1.4 | K08C7.5 | Y39B6A.33 |
| C56C10.8 | ZK622.3 | K11H3.3 | T21E12.4 | ZK973.10 |
| F07A5.7 | DY3.2 | K11C4.3 | T01H3.1 | F32B5.8 |
| F09F7.2 | Y73F8A.6 | F59A2.3 | T09A5.11 | C50F4.8 |
| T01C3.7 | K07E8.3 | K08E3.5 | C34D4.14 | R06F6.11 |

| | | | | |
|---|---|---|---|---|
| C06B8.8 | R07E4.6 | F40F9.6 | K02F3.2 | C10E2.6 |
| C36E6.5 | R09H10.5 | K03C7.2 | T22D1.9 | W09C2.3 |
| C42D8.8 | T20G5.1 | F47B10.1 | Y54F10BM.2 | F08F3.3 |
| Y79H2A.1 | F41H10.7 | F54E2.3 | F16H6.1 | ZK1321.4 |
| B0222.6 | W06A7.3 | ZK1320.2 | C25H3.9 | T14G10.5 |
| C37A2.7 | B0350.2 | W08G11.4 | W05H9.1 | K03A1.2 |
| K09F5.3 | F07B7.5 | F53F4.11 | T07C4.7 | ZK686.3 |
| R05G6.7 | F26E4.9 | F32B5.1 | T12D8.8 | C18E9.4 |
| Y105E8A.16 | Y69H2.14 | T15B7.2 | C12D8.10 | F09F7.6 |
| F56E10.4 | F58D5.1 | B0464.1 | ZK892.2 | F26F4.10 |
| Y65B4BR.5 | C24B9.3 | T08A9.7 | ZK770.3 | F56C9.7 |
| Y49A3A.2 | T05G5.6 | F53F4.10 | F09E5.3 | K10C3.6 |
| T21B10.2 | M02D8.4 | F32A5.4 | C16A3.3 | Y56A3A.32 |
| T02G5.7 | B0546.1 | C34H4.4 | C38C3.5 | B0286.3 |
| W01D2.1 | W02A2.1 | T25B6.2 | T08B1.2 | T07C12.7 |
| C36E6.3 | C16A3.10 | T10C6.11 | ZC15.8 | F42G4.3 |
| W09H1.6 | Y54E2A.11 | W04E12.8 | W06H3.3 | T02B11.4 |
| Y69A2AR.18 | M110.4 | W04C9.1 | Y43C5A.2 | ZK112.2 |
| F22F7.1 | C56G2.1 | F26E4.6 | F25D1.1 | C05C12.4 |
| Y41D4B.5 | C32D5.9 | C17G10.9 | Y67D2.3 | F14F4.3 |
| C55B7.4 | K01G5.4 | Y39E4B.1 | F25H5.1 | K12C11.2 |
| Y5F2A.1 | R12H7.2 | F39B3.3 | F42F12.10 | F58D5.5 |
| F41H10.8 | C15F1.6 | K11E8.1 | T04G9.5 | Y39E4B.3 |
| T28F4.5 | F56B3.1 | F23B2.11 | C46F11.2 | K11G12.5 |
| Y22D7AL.5 | M60.4 | F22D6.2 | T07C4.4 | F54B3.3 |
| W09C5.6 | C34F11.3 | Y73F4A.2 | F55A3.3 | M01A10.3 |
| C44B12.2 | F54A3.3 | DH11.2 | F21F3.1 | Y54H5A.1 |
| F35C5.6 | K07D8.1 | K01C8.9 | Y71H2B.10 | R31.2 |
| F01G10.1 | R04F11.2 | R02D3.1 | Y51A2D.14 | C44F1.3 |
| T08A9.9 | T02B11.3 | C03C10.1 | F45D3.3 | F01F1.9 |
| H03A11.2 | F11E6.5 | H34I24.2 | H16O14.1 | R10E11.8 |
| R11D1.8 | Y105C5A.13 | R03D7.1 | C09D1.1 | B0218.1 |
| Y75B12B.2 | ZC8.4 | T21C9.3 | T01D3.6 | T04A8.7 |
| K10C2.1 | T07A9.9 | C47E12.1 | F48E3.3 | R74.3 |
| F20B6.2 | F53A9.10 | K11H3.1 | Y67H2A.8 | F40F4.4 |
| D1025.6 | C27D11.1 | C49G7.4 | F02G3.1 | Y76A2B.3 |
| F54E7.2 | C28C12.7 | C25B8.3 | F55A8.2 | F57B1.4 |
| F09E5.15 | ZK484.1 | Y50D7A.7 | F22E12.1 | ZK809.3 |
| M117.2 | H14A12.2 | ZC395.10 | F17E9.12 | T02G5.8 |
| C08H9.2 | Y37E3.17 | T28H10.3 | F22B5.9 | Y38F2AR.9 |
| T10E10.2 | C30F8.2 | Y57G11C.24 | F42A8.1 | D2085.1 |
| C47E12.4 | B0403.4 | T27E9.2 | F21A10.2 | F20D6.4 |
| F02E8.1 | F46B6.7 | F57H12.1 | C34B2.8 | F57B9.2 |
| C49G7.3 | T21C12.2 | Y67D8C.5 | Y8G1A.2 | T24H7.5 |
| B0412.4 | C17G10.5 | C18B2.5 | ZC477.9 | F10C1.8 |
| ZK270.2 | Y17G7B.7 | W10G6.3 | Y102A5A.1 | F22B5.2 |

| | | | | |
|---|---|---|---|---|
| T18D3.4 | C10G11.5 | F14E5.2 | F40E10.3 | C18A3.3 |
| F56D2.1 | K08D12.6 | F28B4.3 | C28C12.5 | Y48G8AL.5 |
| C06H2.1 | C15F1.7 | F53F10.4 | B0205.7 | C54D10.3 |
| B0034.3 | C17E4.9 | F01G4.1 | C06A1.1 | Y80D3A.1 |
| F55D10.2 | Y76A2B.5 | K09A9.5 | B0334.1 | R13H8.1 |
| F13D12.4 | R11A8.6 | F27D4.1 | C15H9.1 | F54F2.2 |
| F46E10.10 | Y105E8A.4 | C26C6.2 | H24K24.3 | D2030.4 |
| Y105E8B.1 | F13D12.7 | ZK1058.1 | C37E2.1 | ZC395.5 |
| T10E10.1 | F53F1.4 | W02C12.3 | F44E7.4 | C30C11.2 |
| Y62E10A.1 | C47E12.5 | Y46C8AL.5 | C29E4.8 | Y39B6A.14 |
| E04A4.7 | R12C12.1 | F13H8.7 | Y54F10AM.5 | F47B7.1 |
| C37C3.6 | D1025.7 | Y57A10A.18 | B0035.5 | W09C5.1 |
| F27C1.7 | F46F2.3 | F13D12.6 | W06D4.1 | F59B1.2 |
| T18H9.2 | T24B8.3 | W07E6.1 | C02F4.2 | C16A3.4 |
| R06C1.4 | C09H10.3 | Y71G12B.4 | F33H2.3 | F22H10.3 |
| C49F5.1 | T05H4.12 | T20H4.3 | Y34B4A.6 | Y65B4A.6 |
| ZC410.5 | W06D12.3 | K10C2.3 | T25G3.4 | F53F8.4 |
| F32H2.5 | T02G5.9 | K08F11.3 | Y46G5A.4 | C01G6.5 |
| C14F11.1 | F55H2.2 | F29G6.3 | ZK673.2 | ZC64.2 |

## SUPPLEMENTAL FIGURES

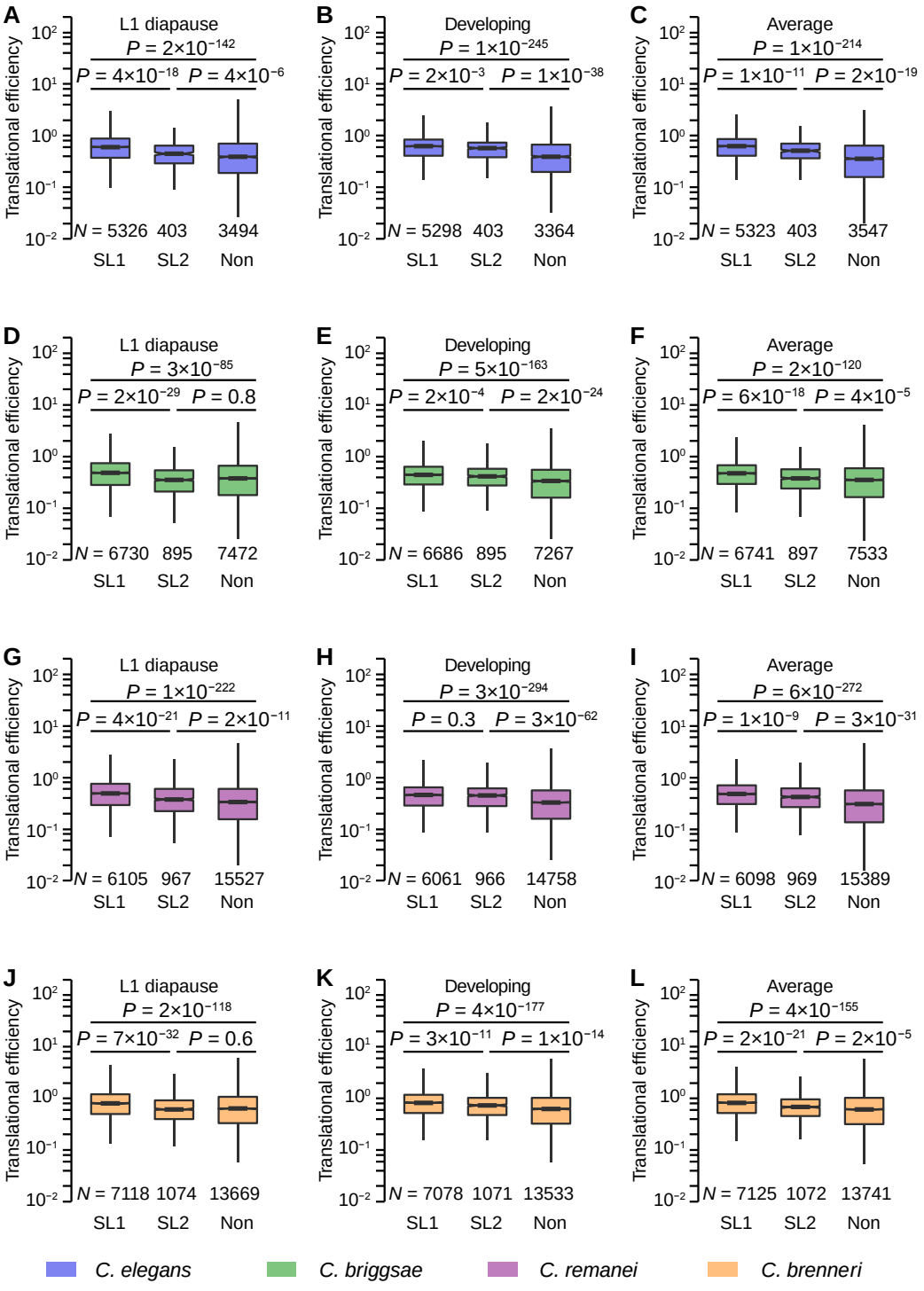


**Fig. S1.** *Trans*-spliced genes exhibit higher translational efficiencies in nematodes. (**A**, **D**, **G**, **J**) Translational efficiencies in L1 diapause worms; (**B**, **E**, **H**, **K** ) translational efficiencies in developing L1 worms; (**C**, **F**, **I**, **L**) average translational efficiencies.

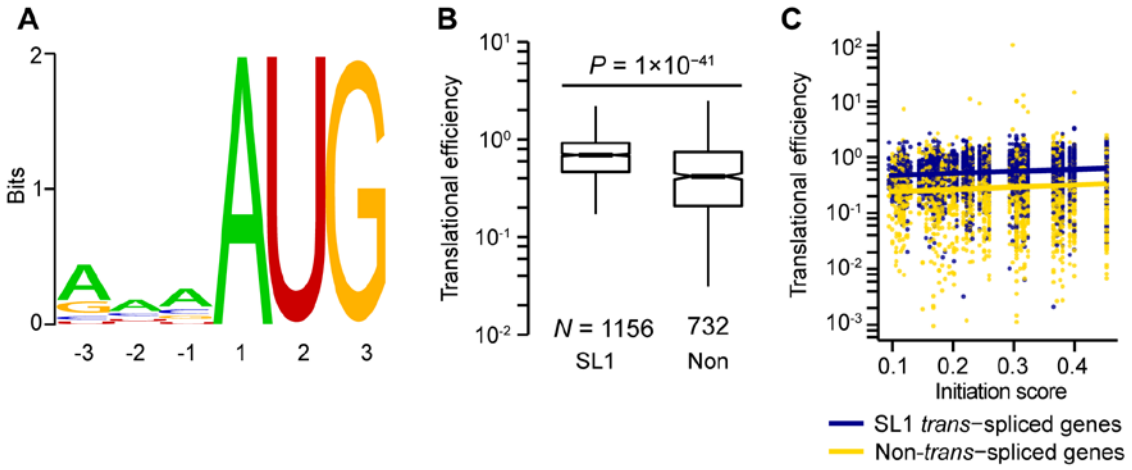


**Fig. S2.** Initiation codon context does not confound our results. (**A**) The Kozak consensus sequence in *C. elegans*. (**B**) SL1 *trans*-spliced genes exhibit higher translational efficiencies than non-*trans*-spliced genes when both are in perfect initiation context (AAAAUG). *P* value was given by the Mann-Whitney *U* test. (**C**) SL1 *trans*-spliced genes still exhibit higher translational efficiencies than non-*trans*-spliced genes after controlling for the initiation score ($P = 6\times10^{-10}$, $N = 8{,}792$, linear regression model: translational efficiency ~ *trans*-splicing + initiation score). The initiation score is positively correlated with translational efficiency ($\rho = 0.14$, $P = 2\times10^{-23}$, $N = 5{,}262$ for SL1 *trans*-spliced genes and $\rho = 0.10$, $P = 4\times10^{-9}$, $N = 3{,}530$ for non-*trans*-spliced genes). Linear regression lines are shown.

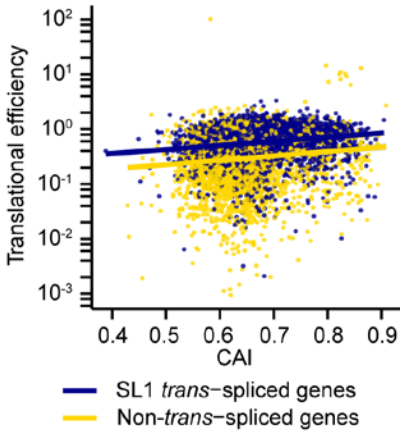


**Fig. S3.** SL1 *trans*-spliced genes still exhibit higher translational efficiencies than non-*trans*-spliced genes after controlling for CAI ($P = 1\times10^{-7}$, $N$ = 8,870, linear regression model: translational efficiency ~ *trans*-splicing + CAI). CAI is positively correlated with translational efficiency ($\rho$ = 0.26, $P = 2.8\times10^{-80}$, $N$ = 5,323 for SL1 *trans*-spliced genes and $\rho$ = 0.14, $P = 2.2\times10^{-17}$, $N$ = 3,547 for non-*trans*-spliced genes). Linear regression lines are shown.

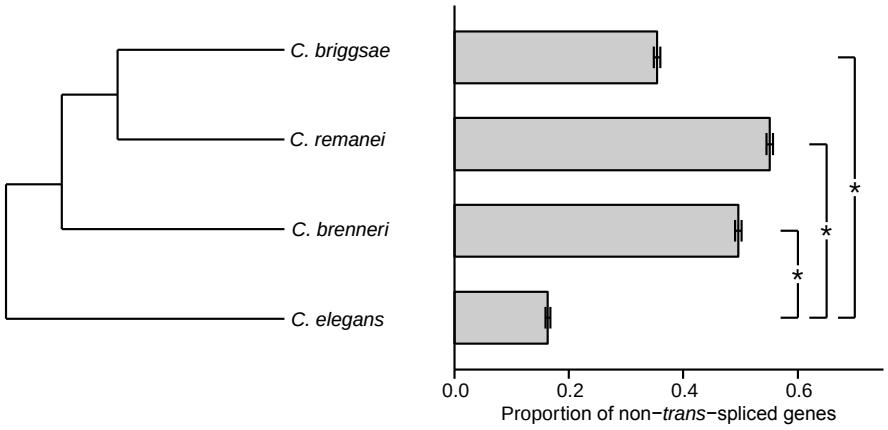


**Fig. S4.** The proportion of non-*trans*-spliced genes is smaller in *C. elegans*.

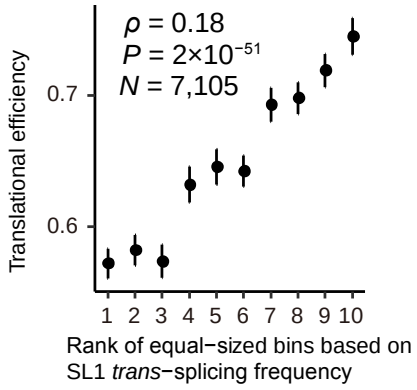


**Fig. S5.** Translational efficiency is positively correlated with SL1 *trans*-splicing frequency in partially SL1 *trans*-spliced genes. A gene was identified as partial SL1 *trans*-spliced if RNA-seq reads supporting both SL1 *trans*-spliced isoform and non-*trans*-spliced isoform exist. The SL1 *trans*-splicing frequency of a gene was defined as the proportion of reads supporting SL1 *trans*-splicing among all reads covering the *trans*-splicing site. Partially SL1 *trans*-spliced genes ($N$ = 7,105) were separated into 10 equal-sized bins. The mean value of translational efficiencies and the standard error of the mean (SEM) within each bin are shown. Spearman's correlation coefficient $\rho$ and the corresponding $P$ value were calculated from unbinned data.

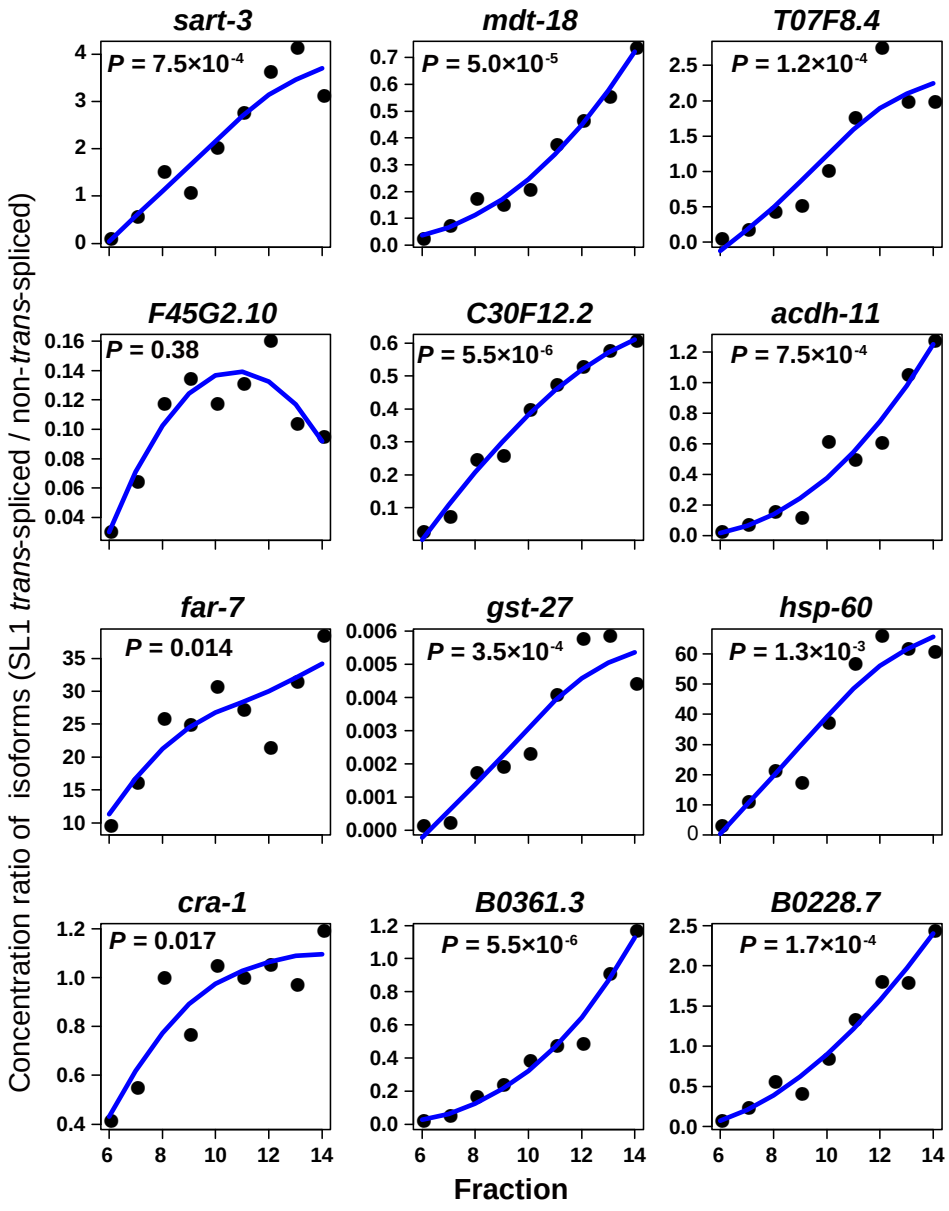


**Fig. S6.** Concentration ratio of two isoforms (SL1 *trans*-spliced / non-*trans*-spliced) is positively correlated with fraction rank in the sucrose gradient centrifugation experiment. An experimental replicate of **Fig. 3C**.

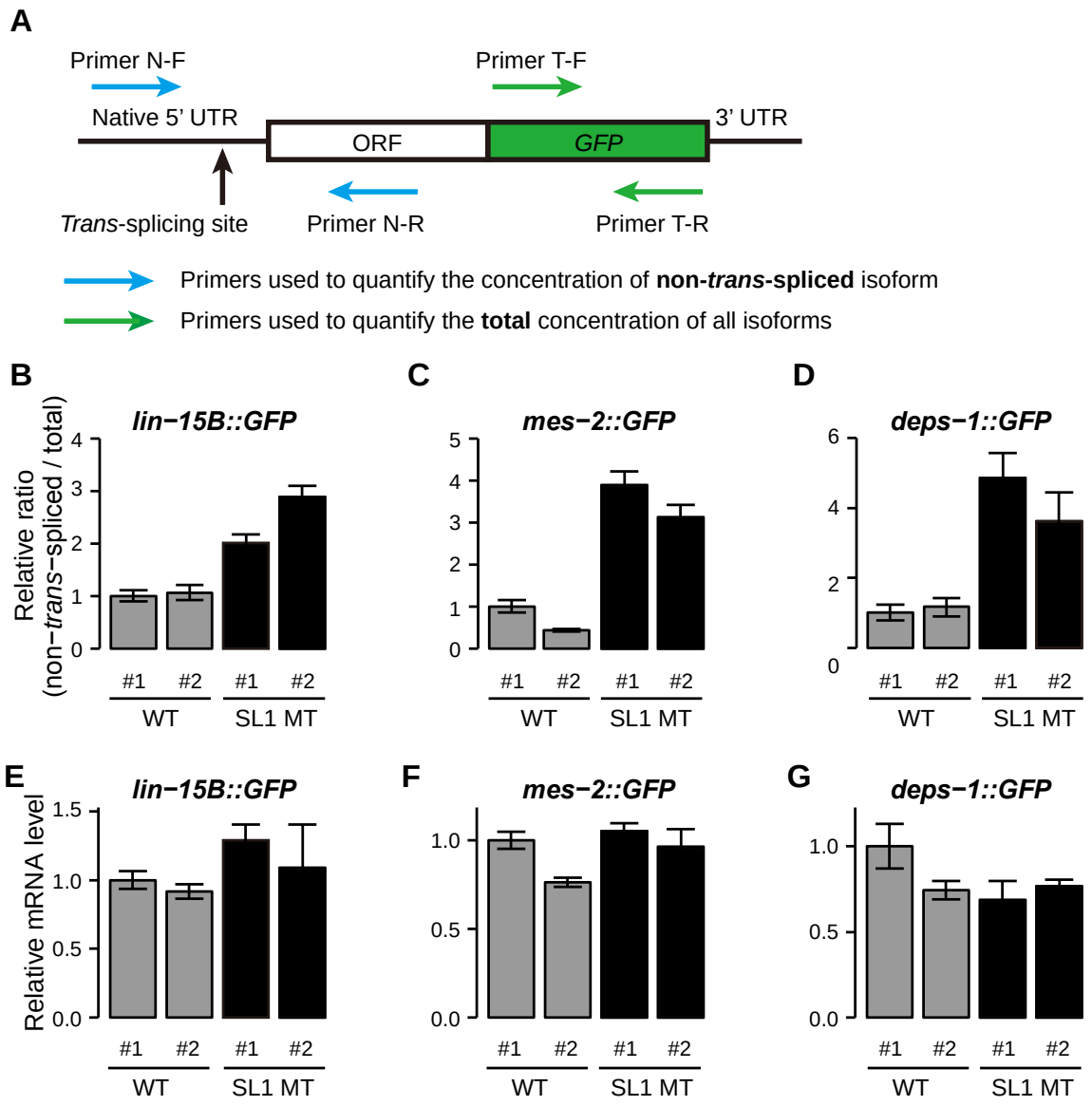


**Fig. S7.** Knocking out the consensus sequence of *trans*-splicing sites leads to reduced *trans*-splicing frequency. (**A**) qPCR primers were designed to quantify the *trans*-splicing frequency and total mRNA level. (**B**-**D**) Knocking out the consensus sequence of *trans*-splicing sites reduces the *trans*-splicing frequencies in *lin-15B* (**B**), *mes-2* (**C**), and *deps-1* (**D**). Two biological replicates (#1 and #2) were performed for each genotype. Error bars represent the standard deviation of three technical replicates. (**E**-**G**) The mRNA levels of *lin-15B* (**E**), *mes-2* (**F**), and *deps-1* (**G**) were normalized to the mRNA level of a tubulin gene (*tba-1*).

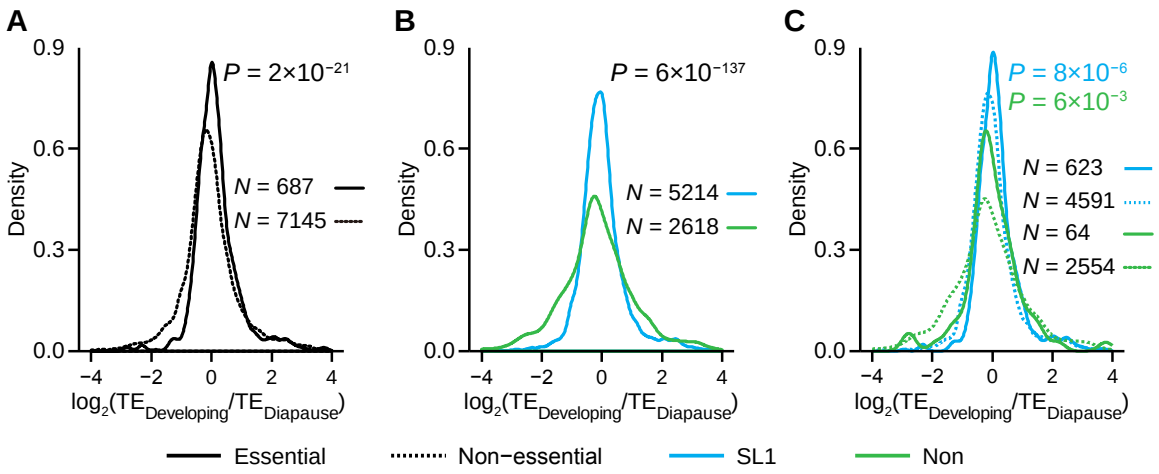


**Fig. S8.** Environmental robustness of translational efficiency is enhanced by SL1 *trans*-splicing. (**A**) Compared to nonessential genes, the translational efficiencies of essential genes are more robust during L1 diapause exit in *C. elegans*. (**B**) SL1 *trans*-spliced genes have more robust translational efficiencies than non-*trans*-spliced genes. (**C**) After controlling for *trans*-splicing type, essential genes still exhibit stronger robustness of translational efficiencies than nonessential genes.

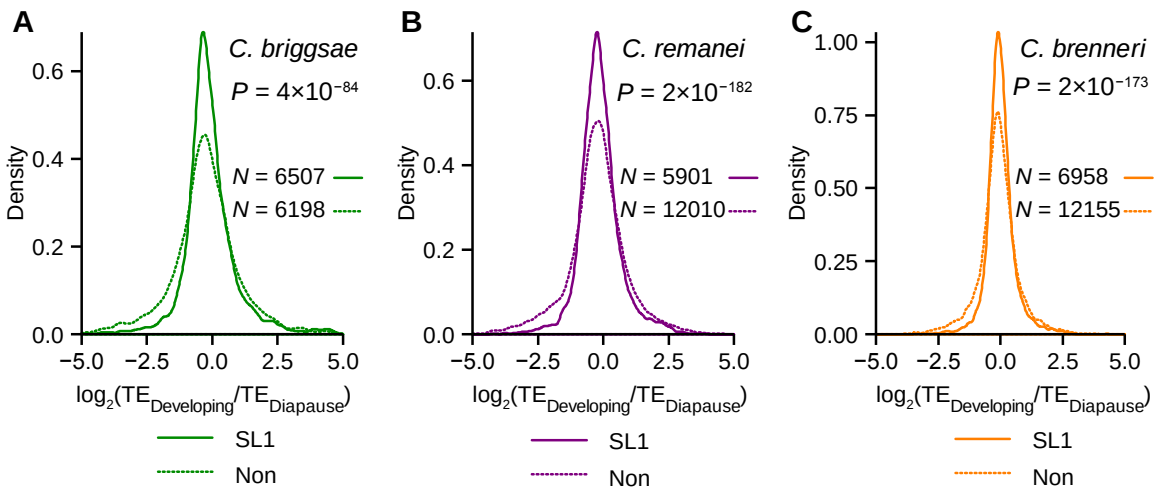


**Fig. S9.** SL1 *trans*-spliced genes have more robust translational efficiencies than non-*trans*-spliced genes during L1 diapause exit in (**A**) *C. briggsae*, (**B**) *C. remanei*, and (**C**) *C. brenneri*. Similar to Fig. **S8B**.